The 9th ALMA Summer School

Polarization Team

Satyajeet Moharana, 서민영, Shan Li, 홍영표

Mentors: Dr. Yusuke Aso, Dr. Bo Huang

📍한국천문연구원

Outline

1 **Introduction**

Dust polarization mechanism

2 **Polarized continuum imaging**

Data reduction Methodology

3 **Result**

Polarization maps and magnetic field morphology

4 **Conclusion**

Summary of the work

1. Introduction: Dust Grain Alignment Mechanism

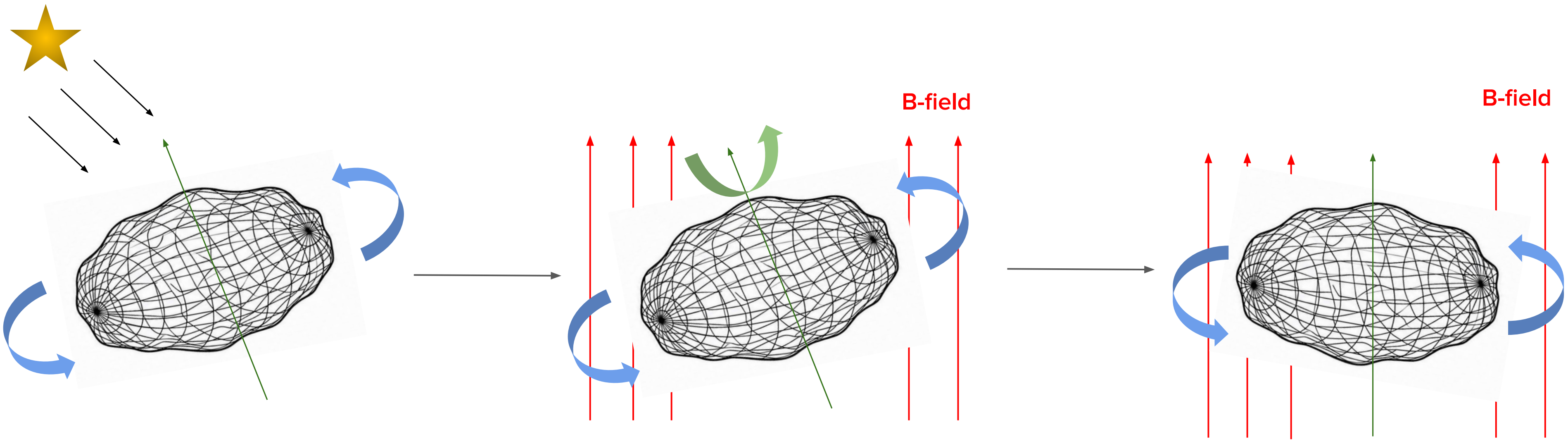

Radiation imparting on an aspherical dust grain causes rotation of the grain due to torque, which becomes maximum when the grain rotates along its minor axis. If the grain is paramagnetic, it will become magnetized along the spin axis.

The ambient magnetic field induces precession on the spinning magnetized dust grain.

The grain becomes stable by aligning its rotation axis (minor axis) with the magnetic field.

1. Introduction: Tracing B-Fields with Dust Polarization

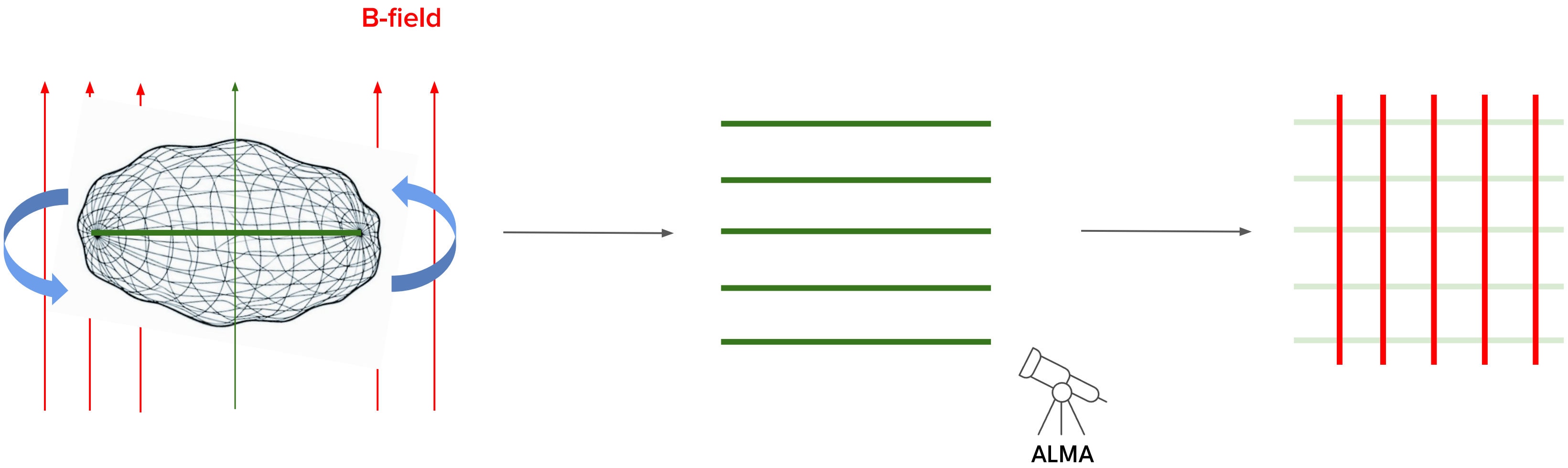

The aligned grains emit polarized emission more strongly along their long axes than that along the short axes.

Polarized signal received by the telescope

The polarization vectors being rotated 90 degrees to infer the ambient magnetic field orientation

1. Introduction: Datasets

- 870 μm (Band 7) Polarimetric observations of 4 protostars within the Orion molecular cloud taken from the BOPS project. *(B. Huang et al. 2024)*
- **Sources:** HH270IRS, HOPS-168, HOPS-169, HOPS-400
- **Resolution:** ~400 au (res. ~ 1 arcsec)
- **Size:** ~3000 au (LAS ~ 8 arcsec)

Name	RA (J2000)	Dec (J2000)	Distance (pc)	Class	L_{bol} ($L_\odot$)	T_{bol} (K)
HH270IRS	05:51:22.72	02:56:04.95	460.0	I	7.00	32.0
HOPS-168	05:36:18.95	−06:45:23.63	383.3	0	48.07	54.0
HOPS-169	05:36:36.17	−06:38:54.46	384.0	0	3.91	32.5
HOPS-400	05:42:45.26	−01:16:13.94	415.4	0	2.94	35.0

2. Polarized continuum imaging

2. Polarized continuum imaging

2.1 Data Inspection: `listobs()`

Band	ALMA 7
Scan	30 seconds x 18
Spectral window	2
Central frequency	~ 345 GHz, ~348 GHz
Correlation products	XX, XY, YX, YY
Antenna diameter	12 m

2. Polarized continuum imaging

2.2 Parameter Estimation: `plotms(... xaxis = 'uvwave', yaxis = 'amp'...)`

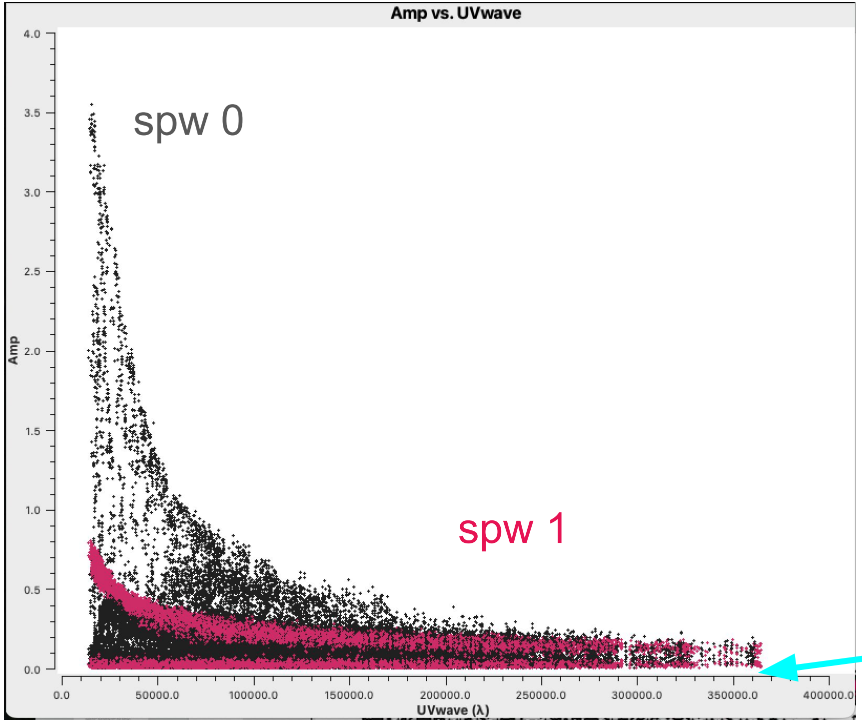

Resolution	1 / max UVwave = 0.573”
FoV	1.13 * λ / D = 18”
Cell size	(1 / 5) * resolution = 0.1”
Map size	2 * FoV / cell size = 360 -> 512 x 512

max UVwave: ~360,000 λ

2. Polarized continuum imaging

2.3 Flagging: `plotms(... xaxis = 'channel', yaxis = 'amp’'...)`

`flagdata(...spw=' 0:0~4, 0:55~75, 1:0, 1:121~127 '...)`

Splitting: split()

flag out emission line data

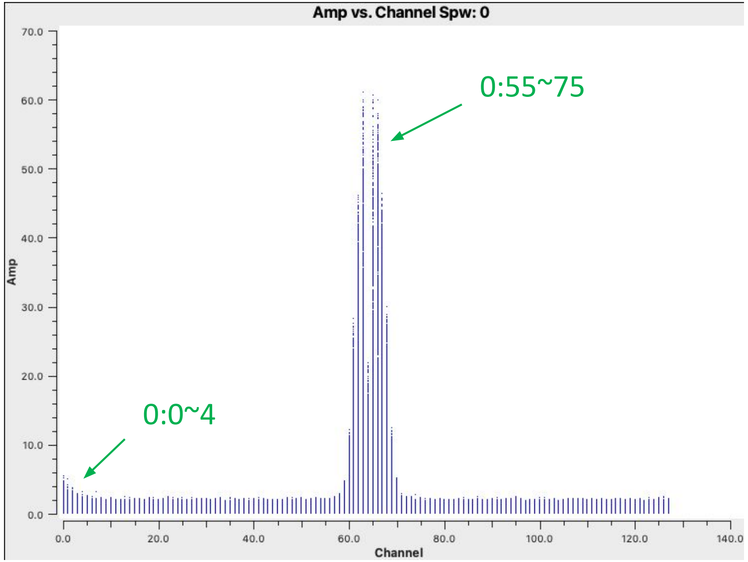

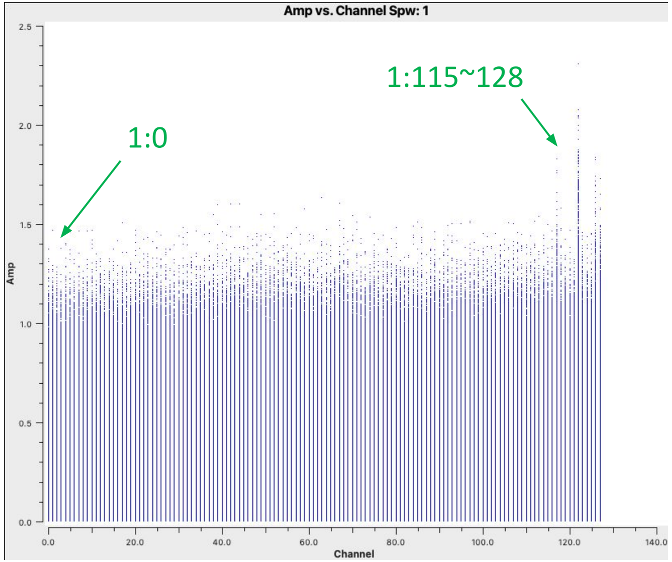

2. Polarized continuum imaging

2.4 CLEAN: `tclean(...imsize= 512, cell= ['0.1arcsec'], spw= '0,1', stokes= 'I', niter=0...)`

Dirty image

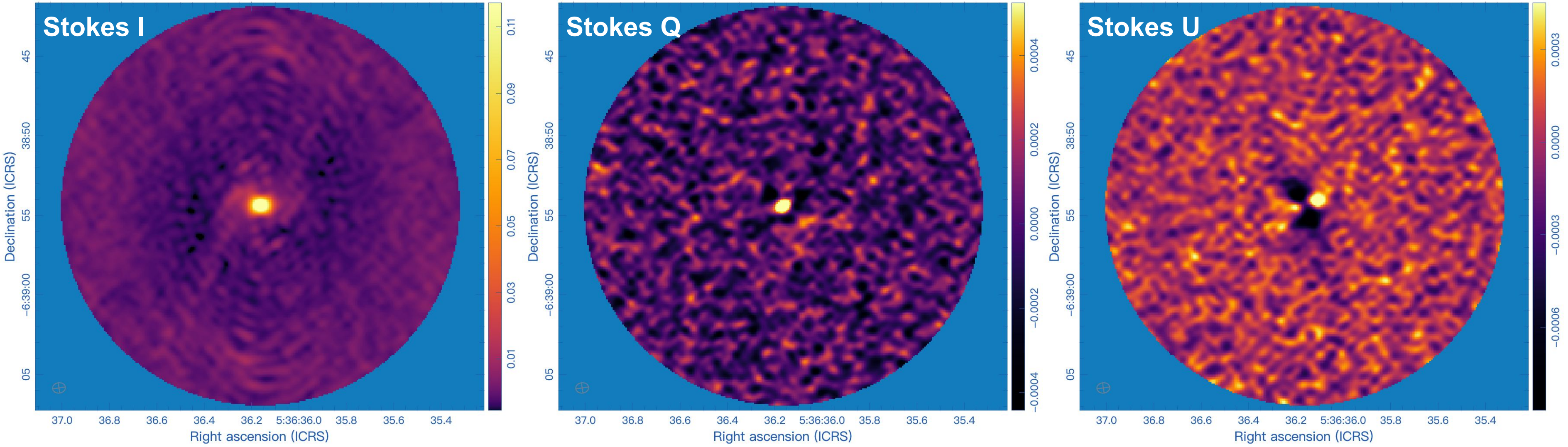

2. Polarized continuum imaging

2.4 CLEAN:
```
tclean(...imsize= 512, cell= ['0.1arcsec'], spw= '0,1',
stokes= 'I', threshold= '2 * rms mJy', pblimit=-1...)
```

CLEAN image

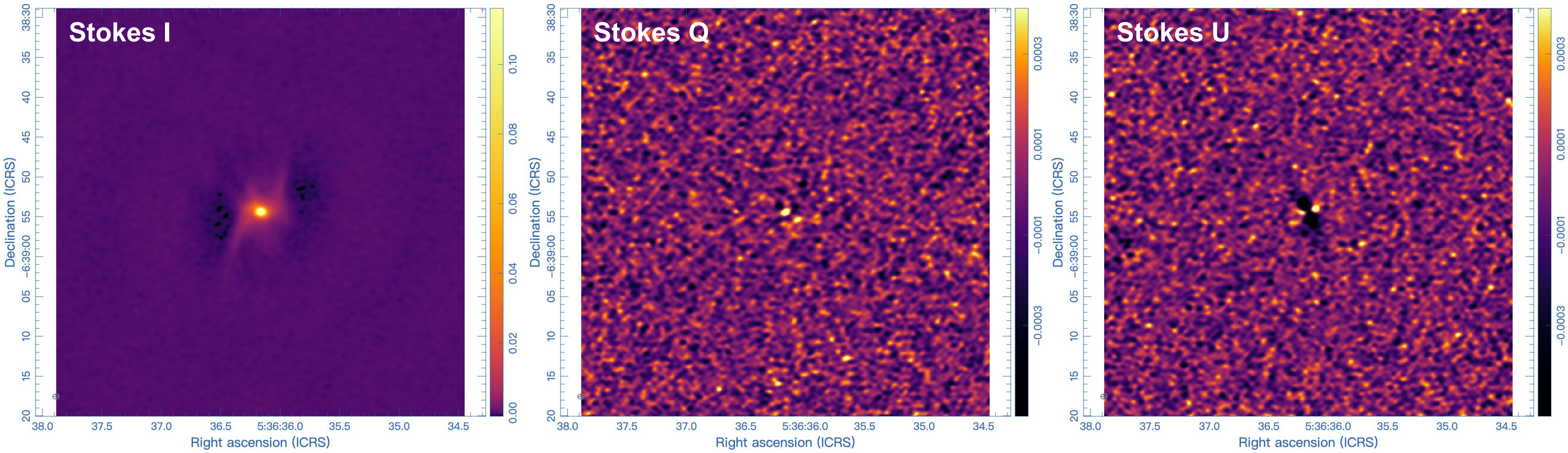

2. Polarized continuum imaging

Polarization intensity image:

```
immath(...mode='poli',
imagename=['StokesQ_image',
sigma='rms_Q/U mJy/beam'...)
```

$$P = \sqrt{Q^2 + U^2 - \sigma_{QU}^2}$$

Polarization angle image:

$$\theta = \frac{1}{2}\arctan\frac{U}{Q}$$

```
immath(...mode='pola',
imagename=['StokesQ_image', 'StokesU_image'],
polithresh='3 * rms_POLI mJy/beam'...)
```

Fractional polarization:

$$P_{frac} = \frac{P}{I}$$

```
immath(...mode='evalexpr',
imagename=['StokesI_image', 'StokesQ_image',
'StokesU_image'],
expr='sqrt((IM1^2+IM2^2-rms_Q/U^2)/IM0^2)'...)
```

CARTA

- Load as hypercube
- Contour (Stokes I)
- Vector overlay

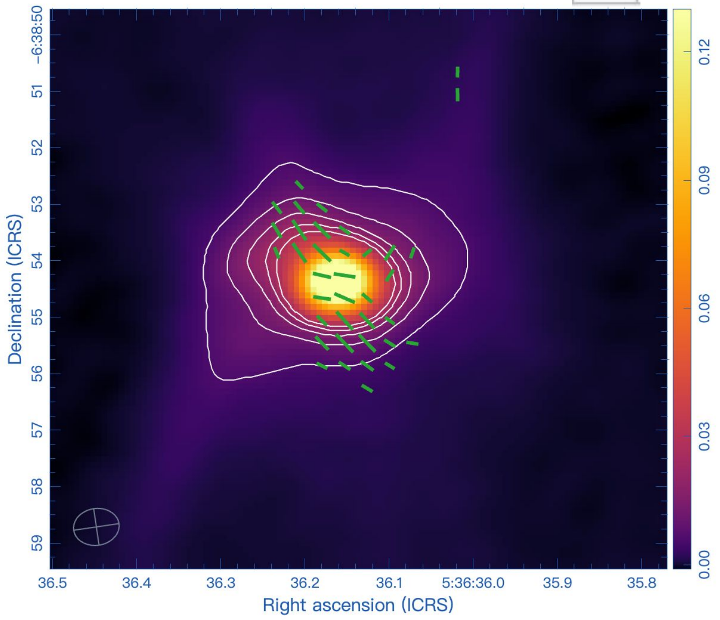

3. Result

Different *tclean* parameter test - ***Weighting***

Higher Sensitivity

Stokes I Intensity

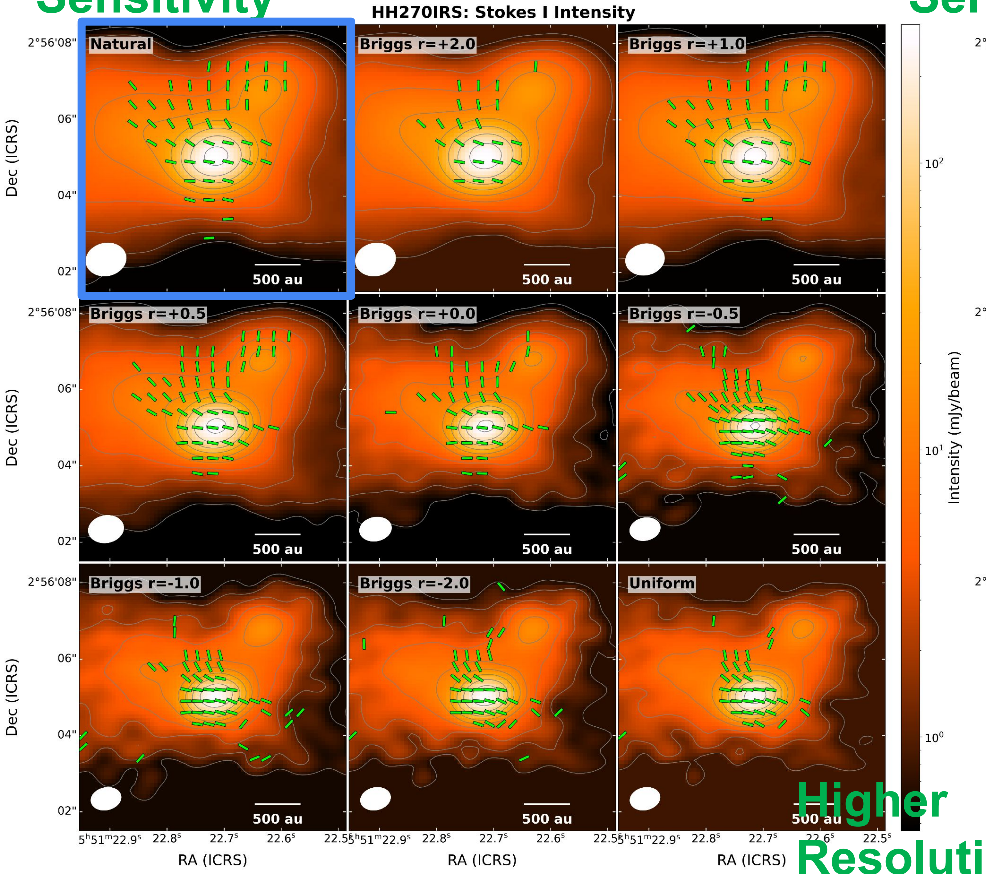

Higher Sensitivity

Polarization Intensity

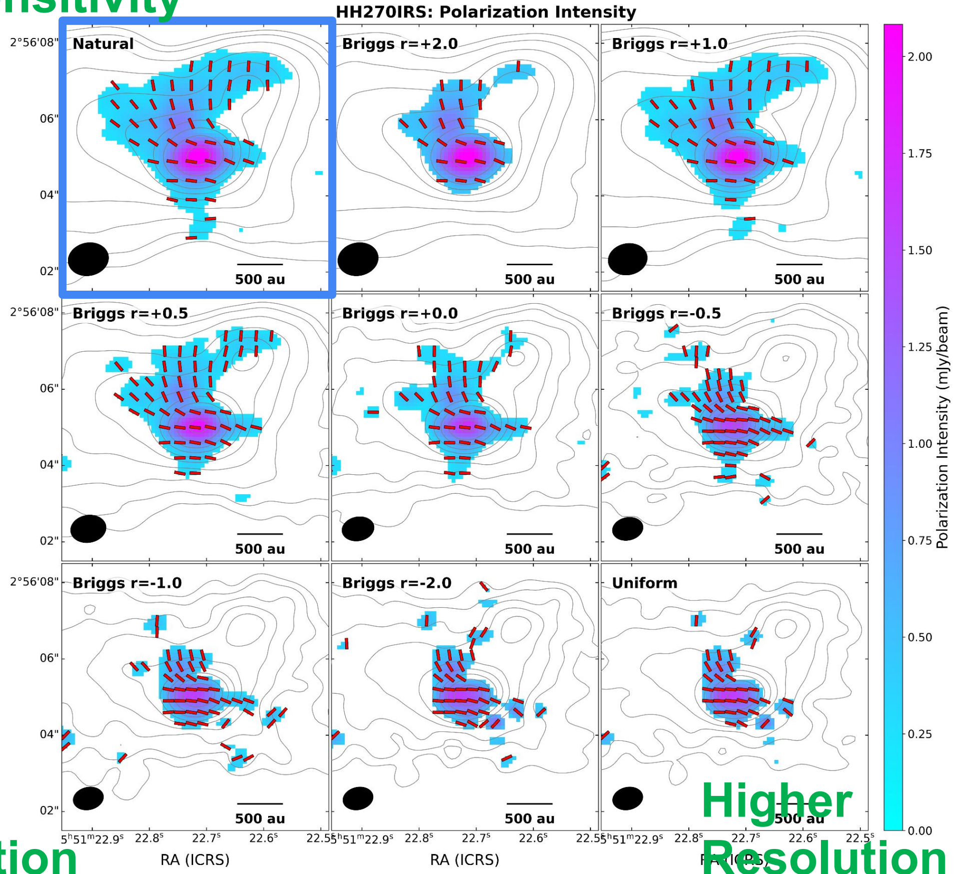

Higher Resolution

Higher Resolution

3. Result

B-field Strength

Davis-Chandrasekhar-Fermi (DCF) Method: $B^{DCF}_{u,pos} \simeq Q^{DCF}_{u,pos} \frac{\sqrt{4\pi\rho}}{\delta\phi} \sigma_{nth}$

: to estimate **magnetic field strength** in space by combining **polarization data** with **gas motion measurements**

$Q^{DCF}_{u,pos}$: Correction Factor ⇨ $Q^{DCF}_{u,pos} \approx 0.5$

ρ : Gas density ⇨ derived from dust emission (Stokes I map)

σ_{nth} : Nonthermal velocity dispersion ⇨ derived from molecular line emission

$\delta\phi$: Measured polarization angle dispersion

⇨ **We can get this value in our data!**

3. Result

1. HOPS-168

- The reduced **I, Q, and U** maps were used to derive the **polarization intensity, angle, and fraction maps** using the standard definitions.
- The **obtained polarization vectors** were rotated by **90 degrees** to infer the **B-field** orientation.

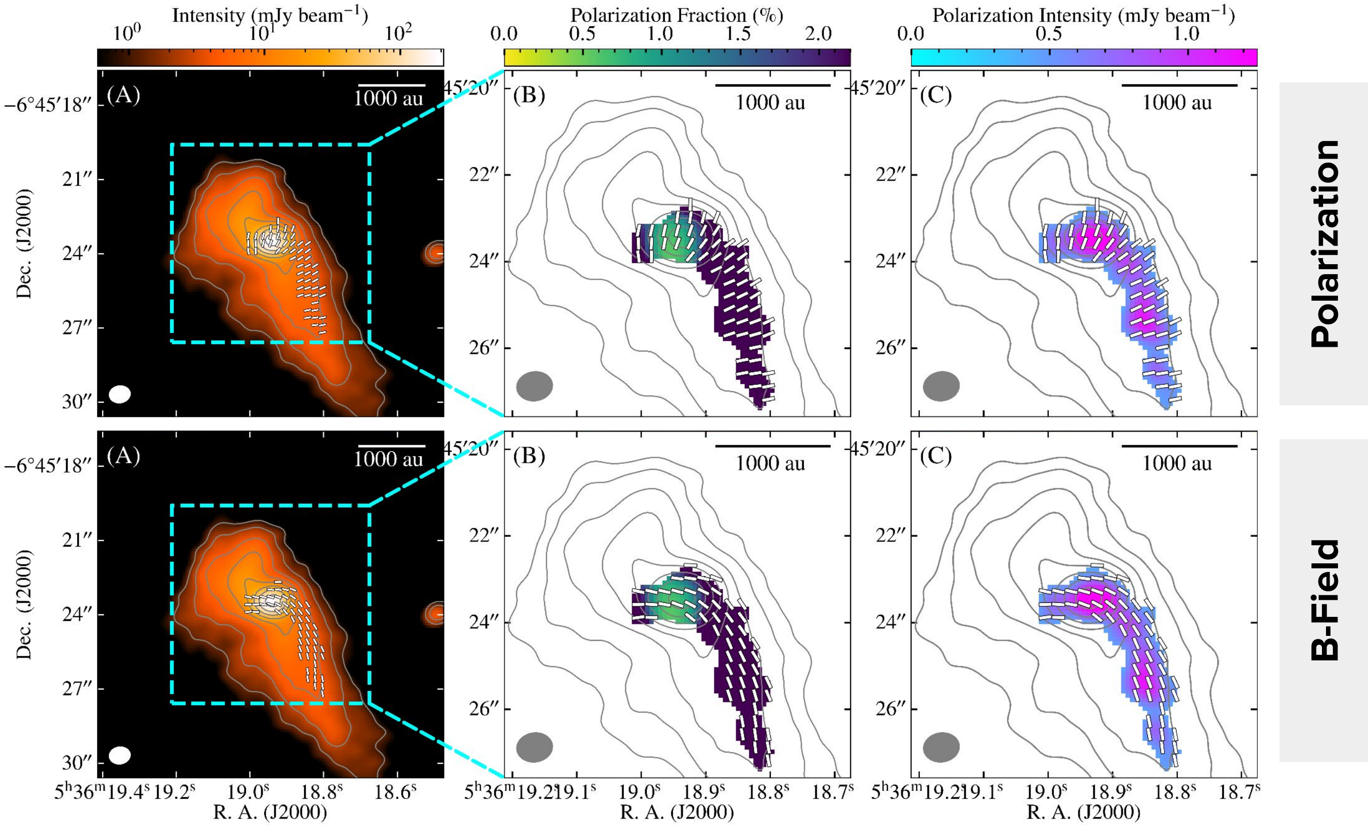

3. Result

4. HH 270IRS

- **Magnetic Field Configuration:**
  A **rotated-hourglass** mor

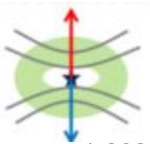

(Huang et al. 2024)

- **Angle Dispersion:**
  33.8 ± 4.1 (Huang et al. (2025))

B-field strength = 0.6 ± 0.2 mG
(Corrected DCF version)
(Huang et al. (2025))

Polarization Direction

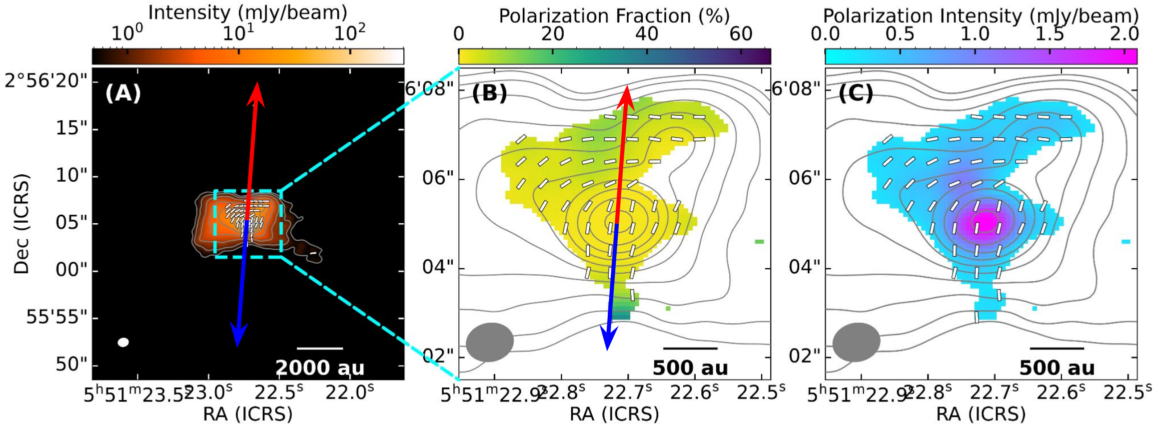

Magnetic Field Direction

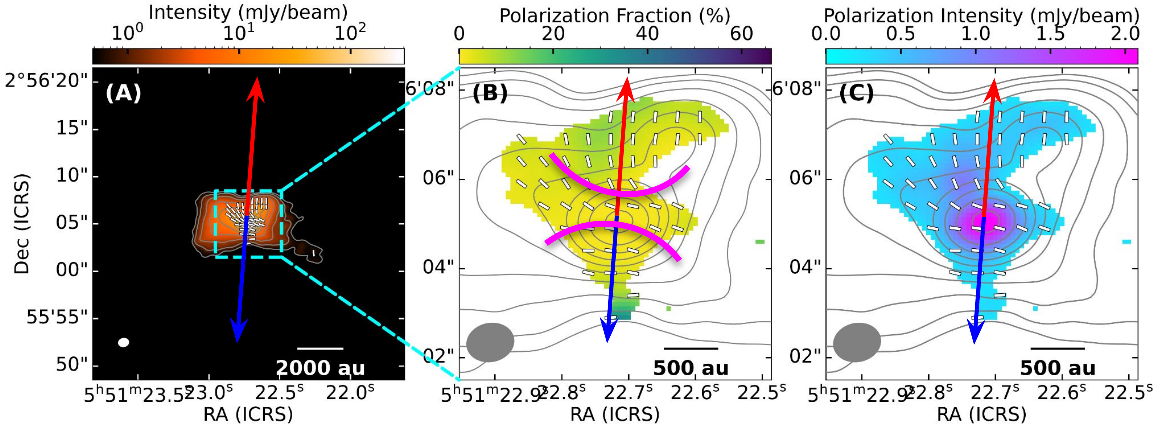

3. Result

1. HOPS-168

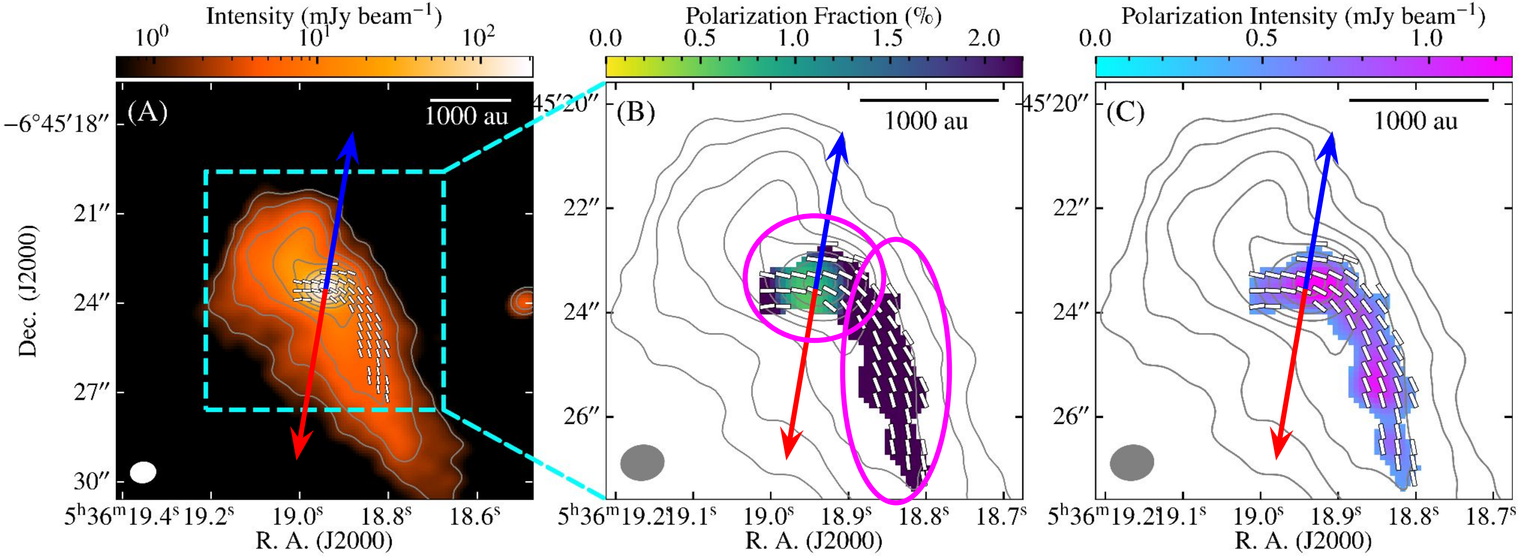

- The **central part** shows an **hourglass** shape, and comparing it with the outflow direction (**B. Huang et al. 2024**), the morphology looks like a **rotated hourglass type**.

(Huang et al. 2024)

- In the **lower** part, the **B-field** looks **parallelly aligned** with the **elongated** structure, likely **tracing** a **streamer-like structure** and **helping** in **gas flow** motions toward the **central** region.
- The **angle dispersion** is **28.4±3.4 degrees** (B. Huang et al. 2025). So we **cannot** use the **standard DCF** method to derive the B-field strength in this region. Using **improved DCF** method with corrections to angle dispersion, the derived **B-field strength** is found to be **0.7±0.4 mG.**

3. Result

2. HOPS-169

Polarization Intensity:
showing **variations** both in **central** and **outer** region.

Polarization fraction:
higher in **outer** part than central region. Related to **aligned-grain polarization**.

B-field orientation:
derived by rotating **polarization** vector by **90°.**

B-field morphology:
ordered and smoothly **curved**.

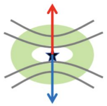

Rotated-hourglass
(Huang et al. 2024)

B-field strength:
0.7±0.2 mG (Huang et al. 2025)

Polarization Direction

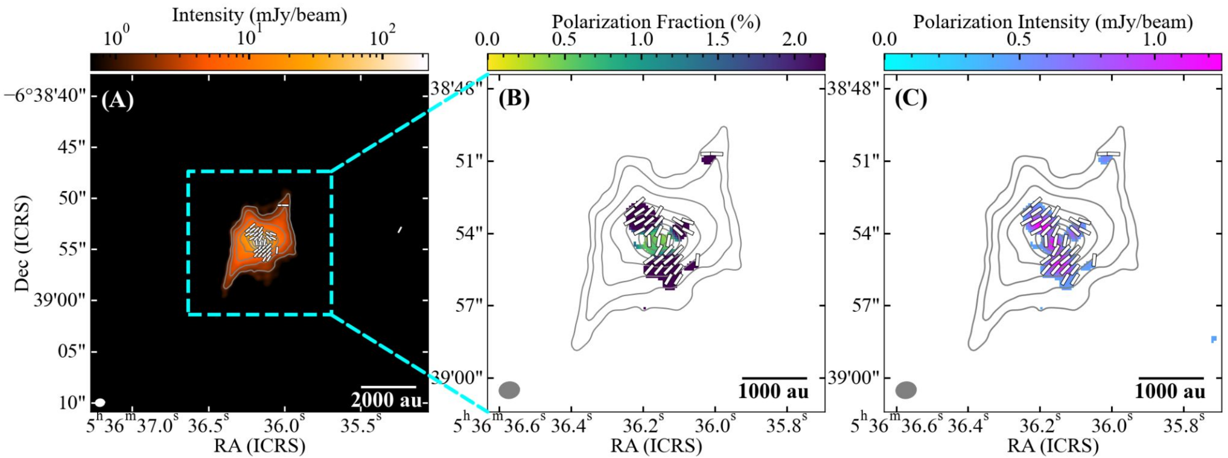

Magnetic Field Direction

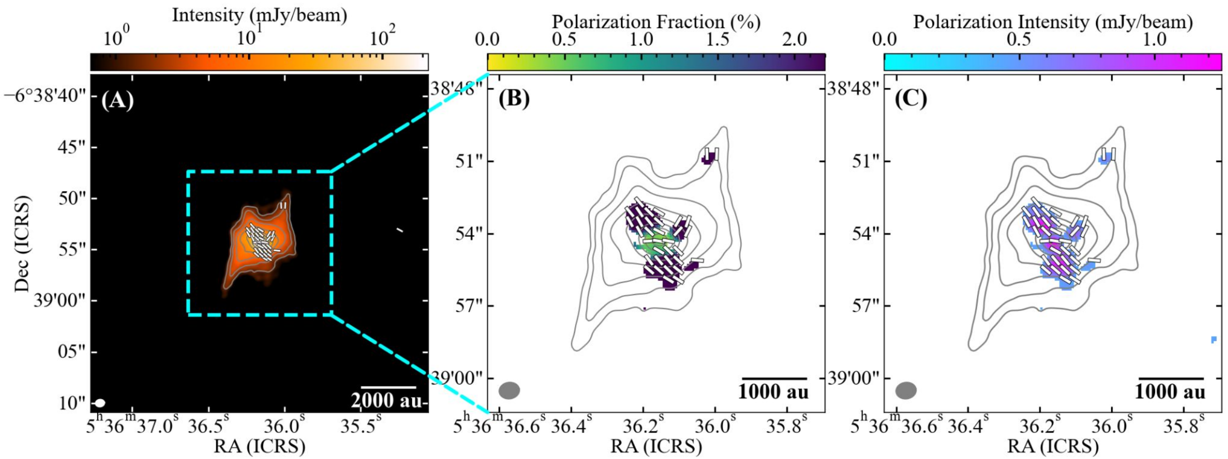

3. Result

3. HOPS-400

B-field strength = 2.1 ± 0.8
(Corrected DCF version)
(Huang et al. (2025)

- **Polarization-B-field relation:**
  The polarization vectors were **rotated** by **90°**

- **B field configuration:**
  A **standard-hourglass** morphology

- **Polarization fraction:**
  Lower polarization fraction near the bright **center**

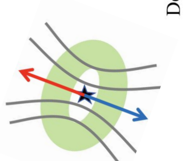

(Huang et al. 2024)

Polarization Direction

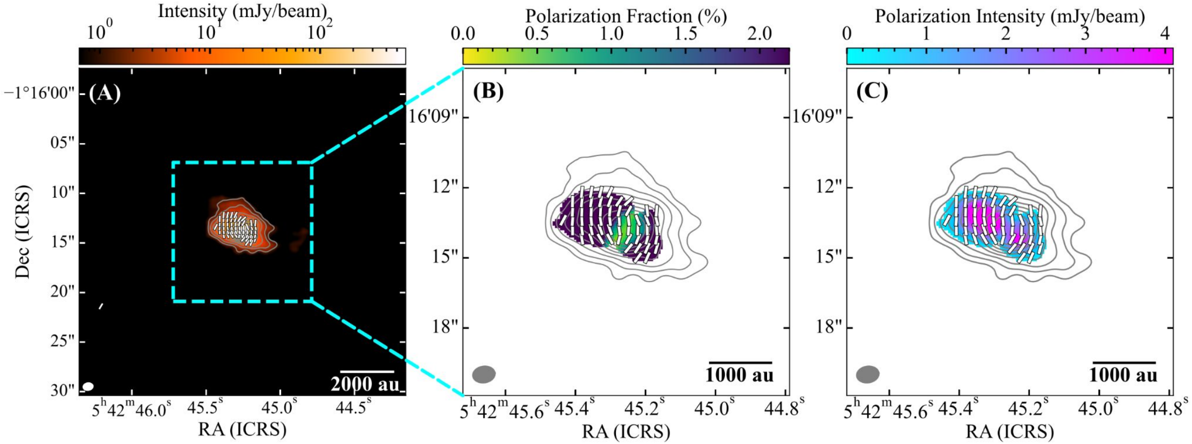

Magnetic Field Direction

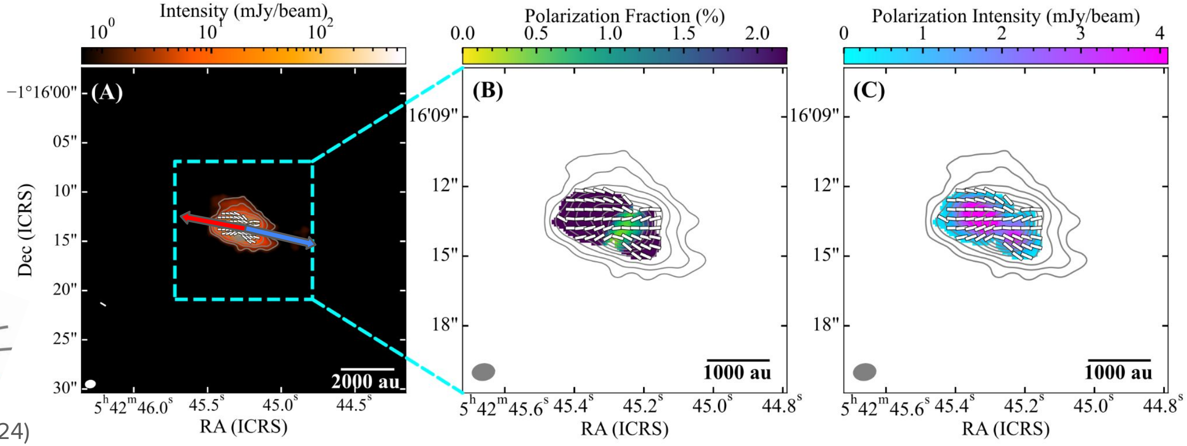

4. Conclusion

- The observation setup and UV coverage were inspected with listobs and plotms.
- The cell and image sizes were set based on the synthesized angular resolution and the primary-beam field of view.
- Line-free channels were extracted using split task.
- tclean reconstructed the sky brightness distribution by deconvolving the synthesized-beam sidelobe from the dirty image.
- Natural gives better sensitivity, uniform gives better resolution, and Briggs balances both using the robust value.
- Stokes I gives total intensity, while Q and U describe linear polarization.
- Polarization intensity shows the strength of polarized emission, polarization angle shows its direction, and polarization fraction is the ratio of polarized intensity to total intensity.
- The plane-of-sky B-field direction was obtained by rotating the polarization vectors by 90°.

Thank You!!


Korea Astronomy and Space Science Institute
한국천문연구원
KASI
9 th
2026
ALMA
Summer
School
27 July
~
31 July
View & Histo

Appendix

Huang et al. (2025)

	1. HH 270IRS	2. HOPS-168	3. HOPS-169	4. HOPS-400
ρ	$2.8 \times 10^{-17} g\ cm^{-3}$	$1.4 \times 10^{-17} g\ cm^{-3}$	$3.9 \times 10^{-17} g\ cm^{-3}$	$8.3 \times 10^{-17} g\ cm^{-3}$
σ_{nth}	$0.42 \pm 0.10 km\ s^{-1}$	$0.51 \pm 0.15 km\ s^{-1}$	$0.39 \pm 0.09 km\ s^{-1}$	$0.40 \pm 0.12 km\ s^{-1}$

Imaging code:
https://dataverse.harvard.edu/dataset.xhtml?persistentId=doi:10.7910/DVN/9HVOZN